

## Collision Properties of Ultracold $^{133}\text{Cs}$ Atoms

Paul J. Leo, Carl J. Williams, and Paul S. Julienne

*Atomic Physics Division, National Institute of Standards and Technology, Gaithersburg, Maryland 20899*  
(Received 25 April 2000)

We present a theoretical analysis of numerous magnetically tunable Feshbach resonances measured by Chin *et al.* [preceding Letter, Phys. Rev. Lett. **85**, 2717 (2000)] at fields of up to 25 mT. This analysis provides the most accurate characterization of the collisional properties of ground state Cs atoms currently available and clearly shows, in contrast to previous work, that Bose-Einstein condensation of  $^{133}\text{Cs}$  cannot be ruled out. The  $X^1\Sigma_g^+$  and  $a^3\Sigma_u$  scattering lengths are constrained to  $(280 \pm 10)a_0$  and  $(2400 \pm 100)a_0$ , respectively ( $a_0 = 0.0529177$  nm), and the van der Waals  $C_6$  coefficient to  $6890 \pm 35$  a.u. (1 a.u. =  $0.0957345 \times 10^{-24}$  J · nm<sup>6</sup>).

PACS numbers: 34.50.-s, 03.75.Fi, 32.80.Pj, 34.20.Cf

This Letter analyzes detailed new data of magnetically tunable Feshbach resonances reported in the accompanying paper [1]. We conclude that the scattering length for  $^{133}\text{Cs}(f = 4, m_f = 4)$  is *positive*  $(2400 \pm 100)a_0$  ( $a_0 = 0.0529177$  nm), contrary to previous reports [2,3], and that  $^{133}\text{Cs}(f = 3, m_f = |3|)$  possesses suitable scattering properties for Bose-Einstein condensation (BEC) for some values of the magnetic field  $B$ . The results described here are quantitative and predictive and fully characterize the threshold scattering properties of  $^{133}\text{Cs}$ .

Ultracold experimental collisional studies of Cs are motivated by attempts at BEC [4–8] and by measurements of collisional clock shifts [9,10] resulting from the unique role Cs plays as a time and frequency standard. These data have been analyzed in previous attempts to determine the singlet  $a_S$  and triplet  $a_T$  scattering lengths, the van der Waals coefficient  $C_6$ , and the second-order spin-orbit interaction. Based on  $(4,4) + (4,4)$  collisional data [4,5], we predicted that the magnitude  $|a_T| > 600a_0$  [11]. In contrast, Ref. [2] obtained  $a_S = (-208 \pm 17)a_0$  and  $a_T = (-350 \pm 35)a_0$  using all the data then available, including collisional clock shifts. Here we label collisions between atoms “ $a$ ” and “ $b$ ” using  $(f_a, m_a) + (f_b, m_b)$  where  $f_\alpha$  ( $\alpha = \{a, b\}$ ) is the atomic hyperfine quantum label with projection  $m_\alpha$ . Our evaluation of the data used in Ref. [2] produces significantly less restrictive results with  $a_T < -350a_0$  or  $a_T > 1000a_0$  and  $a_S \approx -250a_0$  or  $+250a_0$  depending on the value of  $C_6$ . Reference [3] also found that the sign of  $a_T$  depended on the value of  $C_6$  but ultimately found  $C_6 = 6510 \pm 70$  a.u. and a negative value for  $a_T$ .

We model the resonances observed by [1] using a coupled channel theoretical model similar to that described in Refs. [11,12] which uses the fitting parameters:  $a_S$ ,  $a_T$ ,  $C_6$ , and a scaling factor  $S_C$  which controls the strength of the second-order spin-orbit interaction. To represent the interaction between the two colliding  $^2S$  atoms for internuclear distances  $R < 18a_0$  the model uses the  $a^3\Sigma_u$  and  $X^1\Sigma_g^+$  adiabatic Born-Oppenheimer potentials of [13]. Because these short-range potentials are not known with sufficient accuracy to predict ultracold

scattering properties, they are individually modified using the procedure described in [11] to provide an independent means of varying  $a_S$  and  $a_T$  for a given value of  $C_6$ . For larger  $R$  a combination of exchange and a multipolar expansion including retardation corrections is used. We use the exchange potential  $V_{\text{ex}} \propto R^{5.543} \exp(-1.07R)$  from Ref. [14], the retardation corrections  $y_n$  in Ref. [15], and the  $C_8 = (9.546 \times 10^{-5} \text{ a.u.})a_0^2$  and  $C_{10} = (1.358 \times 10^{-8} \text{ a.u.})a_0^4$  coefficients of Ref. [16]. We allow  $C_6$  to vary in a range loosely bounded by the values of Marinescu [17] and Derevianko [18]. Uncertainties in  $C_8$ ,  $V_{\text{ex}}$ , retardation, and the shapes of the Born-Oppenheimer potentials for  $R < 18a_0$  are incorporated into our final estimates of uncertainties in  $a_S$ ,  $a_T$ ,  $C_6$ , and  $S_C$ . The small experimental uncertainties in the resonance positions are negligible when compared to the systematic uncertainties in the theoretical model.

The second-order spin-orbit interaction which controls spin relaxation rates in Cs is modeled using the *ab initio* parametrization of Ref. [12], appropriately scaled to reproduce the experimental data. Both Refs. [2] and [11] have previously shown that the parametrization of Ref. [12] needs to be scaled by a factor of  $\approx 4$ . Here, we treat the scaling factor  $S_C$  as an unknown parameter to be fitted using the accompanying experimental data [1].

Resonances in this paper are labeled with the quantum numbers  $(f, l)$  of the exit channel, where  $l$  is the orbital angular momentum of the colliding atoms [12] and  $f$  is the total hyperfine quantum number given by  $\vec{f} = \vec{f}_a + \vec{f}_b$ . These quantum numbers are not strictly conserved, but remain good approximate quantum numbers for  $B < 25$  mT and help to identify the nature of the coupling of the resonant channel to the entrance channel. For example, when  $(f, l)$  of the entrance and resonant channel are identical the interaction is due to exchange forces, while when they differ the interaction is due to relativistic spin-dependent forces. The contribution of higher partial-wave entrance channels to the resonances studied here are negligible, and within our final uncertainties thermal averaging of the theoretical results does not modify the magnetic field position of the resonances.

The four parameters  $a_T$ ,  $a_S$ ,  $C_6$ , and  $S_C$  in our model are completely constrained by fitting the experimentally observed minima in the  $(3,3) + (3,3)$  elastic cross section  $\sigma_{3,3}^{\text{el}}(B)$  at  $1.7064 \pm 0.0056$  mT and  $4.8017 \pm 0.0032$  mT and the observed position of resonances in the  $(3,-3) + (3,-3)$  and  $(4,-4) + (4,-4)$  inelastic rate at  $3.0051 \pm 0.0056$  mT and  $20.5029 \pm 0.0040$  mT, respectively [1]. Only four resonances are required to constrain the four parameters, and in general we could replace any one of the resonances mentioned above with another resonance possessing similar properties and dependencies on  $a_T$ ,  $a_S$ ,  $C_6$ , and  $S_C$ . We find that one of the resonances must be independent of  $a_S$  (i.e., a pure triplet resonance) in order to prevent tradeoffs among the parameter set. We first find values of  $a_T$  and  $a_S$  which reproduce the minimum in  $\sigma_{3,3}^{\text{el}}(B)$  at  $1.7064 \pm 0.0056$  mT for specified values of  $S_C$  and  $C_6$ . Fitting the second observed minima  $\sigma_{3,3}^{\text{el}}(4.8017 \pm 0.0032$  mT) then fixes the values of  $a_T$  and  $a_S$  given the above values of  $S_C$  and  $C_6$ . We then vary  $S_C$  in order to fit the observed position of the inelastic  $(3,-3) + (3,-3)$  resonance at  $3.0051 \pm 0.0056$  mT and repeat the above steps to fit  $a_T$  and  $a_S$ . In fact, all experimentally observed  $\sigma_{3,3}^{\text{el}}(B)$  minima and all inelastic  $(3,-3) + (3,-3)$  resonances can be fit using only  $a_T$ ,  $a_S$ , and  $S_C$ . To constrain the last model parameter  $C_6$  a pure triplet resonance was needed and the experimentalists [1] found us a  $(4,-4) + (4,-4)$  resonance at  $20.5029 \pm 0.0040$  mT.

Figure 1 shows the calculated  $\sigma_{3,3}^{\text{el}}(1.7064$  mT) for  $C_6 = 6500$  a.u. and  $S_C = 4.0$  at a collision energy  $E/k_B = 1 \mu\text{K}$  where  $k_B$  is Boltzmann's constant. This figure is the starting point for our fitting procedure. The figure is labeled using scaled triplet and singlet scattering lengths defined by  $A_{\{S,T\}}^s = \frac{2}{\pi} \tan(a_{\{S,T\}}/L)$  which map  $-\infty < a_{\{S,T\}} < +\infty$  to  $-1 < A_{\{S,T\}}^s < 1$  where the scaling length  $L = 100a_0$  ( $\approx \frac{1}{2} \sqrt{2\mu C_6/\hbar^2}$ ) and  $a_{\{S,T\}}$  is in

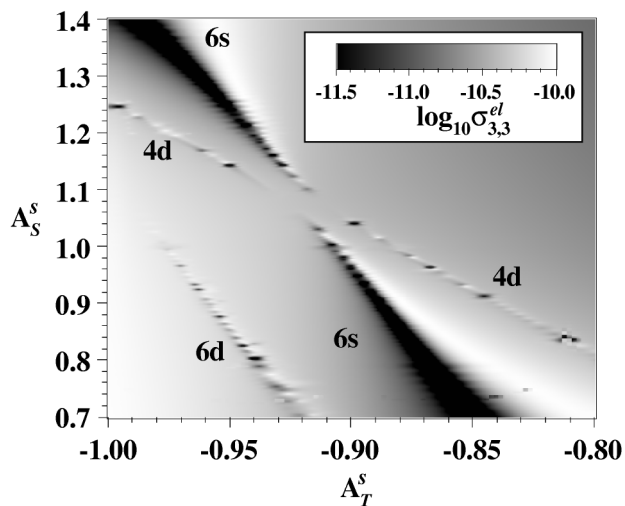


FIG. 1.  $\sigma_{3,3}^{\text{el}}(1.7064$  mT) ( $\text{cm}^2$ ) at  $E/k_B = 1 \mu\text{K}$  for  $C_6 = 6500$  a.u. and  $S_C = 4$  vs  $A_S^s$  and  $A_T^s$  (as defined in the text).

$a_0$ . Note in Fig. 1 we have set  $A_S^s < 0$  to  $A_S^s = A_S^s + 2$  because  $A_{\{S,T\}}^s$  is a periodic function modular 2.

The broken features in Fig. 1, labeled  $4d$  and  $6d$ , are continuous and all coarseness results from the finite resolution of the grid used for  $A_T^s$  and  $A_S^s$ . In the broad dark diagonal band of Fig. 1 the magnitude of the scattering length for the  $6s$  entrance channel at  $B = 1.7064$  mT approaches zero. The narrower dark diagonal minima labeled  $6d$  and  $4d$  are due to Feshbach resonances. At  $A_S^s \approx 1.1$  the  $4d$  resonance appears to the left of the  $6s$  feature and the  $6d$ -resonance is shifted off the left of the figure to positive values of  $A_T^s$ . The details of how these features shift for different  $C_6$ ,  $B$ , and  $S_C$  within such maps is too lengthy to report here. In summary, if  $C_6$  is increased, the features move from right to left. Increasing  $B$  shifts features due to collisions between atoms in high field (low field) seeking states from right to left (left to right). In the above cases the relative positions of features remain unchanged. For example, in Fig. 1, which is a high field seeking case, all features move from right to left as  $B$  increases. A similar map exists for the low field seeking  $(3,-3)$  atoms where the features in  $\sigma_{-3,-3}^{\text{el}}(B)$  will be shifted from left to right relative to those shown in Fig. 1. Modifying the second-order spin-orbit interaction using  $S_C$  shifts resonances caused by relativistic spin-dependent interactions. In Fig. 1 increasing  $S_C$  shifts the  $6d$  and  $4d$  resonances farther apart so that both minima would appear to move farther away from the  $6s$  minima for  $A_S^s < 1.1$ .

The width of the  $\sigma_{3,3}^{\text{el}}(1.7064$  mT) minimum measured in Refs. [1,8] constrains  $a_S$  and  $a_T$  to values in the center of the broad  $6s$  minimum shown in Fig. 1. A second  $6s$  minima in  $\sigma_{3,3}^{\text{el}}(B)$  exists in another region of the  $a_S$  vs  $a_T$  parameter space but is excluded by the other experimental data. The measurement of the second narrow ( $4d$ ) minimum at  $4.8017$  mT [1] is a key component of our fitting procedure, since it excludes the area above  $A_S^s \approx 1.1$  where the narrow  $4d$  minimum appears for  $B < 1.7064$  mT. This immediately constrains  $a_S$  to be either large and positive or  $a_S < -790a_0$  for the range of  $C_6$  we have investigated and excludes those reported in Ref. [2]. For the *specific* values of  $C_6$  and  $S_C$  used in Fig. 1 the relative position of these two measured minima constrains the fit to a point given by  $a_S = (329 \pm 4)a_0$ ,  $a_T = (-486 \pm 4)a_0$ . However, varying the magnitude of the second-order spin-orbit interaction changes the position of the  $4d$  minimum and the fit point shifts on the order of  $300a_0$ , and changing  $C_6$  causes even larger shifts.

By also fitting the  $6d$ -resonance in the  $(3,-3) + (3,-3)$  inelastic rate measured at  $3.0051$  mT [1,8] we can constrain  $S_C$ . The actual fitting procedure is iterative since modifying  $S_C$  also causes the previously fit  $\sigma_{3,3}^{\text{el}}(4.8017$  mT)  $4d$  minima to shift. Fitting to both the  $6d$ -resonance in the  $(3,-3) + (3,-3)$  inelastic rate and the  $\sigma_{3,3}^{\text{el}}(1.7064$  mT)  $6s$  minima is relatively insensitive to the values of  $a_S$  and  $a_T$  over a range of several hundred  $a_0$  because these two features are nearly parallel to each

other in the  $a_S$  vs  $a_T$  parameter space. It is the movement of the  $\sigma_{3,3}^{e1}(4.8017 \text{ mT})$   $4d$  minimum which actually constrains  $a_S$  and  $a_T$  as  $S_C$  varies. This procedure yields  $S_C = 3.2 \pm 0.05$  reducing the magnitude of the second-order spin-orbit interaction from that given in Fig. 1 and reported in Ref. [11]. This shifts the  $4d$ -resonance in Fig. 1 closer to the  $6s$  minima for  $A_S^s < 1.1$  and constrains  $a_S = (254 \pm 4)a_0$  and  $a_T = (-452 \pm 4)a_0$  for  $C_6 = 6500 \text{ a.u.}$

Figure 2 shows how the above fit using  $C_6 = 6890 \text{ a.u.}$  reproduces all  $(3, -3) + (3, -3)$  inelastic resonances. The results show a remarkable agreement with the experimental measurements of [1] for both the shape and positions of the Feshbach resonances. Preliminary zero-field labels are given to the resonances. Not labeled are broad  $6s$  resonances at 8 and 95 mT which are observable at lower collision energies. In this particular experiment the sample contained 95%  $(3, -3)$  and 5%  $(3, -2)$  atoms. The  $(3, -3) + (3, -2)$  resonances at  $\approx 11.0, 12.0, 13.0,$  and  $14.8 \text{ mT}$  were reproduced by the numerical simulation without any further fitting. Figure 2 uses  $C_6 = 6890 \text{ a.u.}$ ; however, similar quality fits for this data set were found for values of  $C_6$  from 6500 to 6950 a.u. In this range of  $C_6$ ,  $a_S$  changes by up to  $50a_0$  and  $a_T$  ranges from  $-450a_0$  to  $1400a_0$  changing from  $-\infty$  to  $+\infty$  at  $C_6 \approx 6802 \text{ a.u.}$

Repeating the procedure above for a range of  $C_6$  values provides a series of parameter sets ( $a_T, a_S, S_C$ ) which provide fits to the  $f_a = 3$  and  $f_b = 3$  resonances, similar to those in Fig. 2. As  $C_6$  does not modify the relative position of  $s$  and  $d$  wave resonances no further fitting of  $S_C$  is required. For  $C_6$  in the range  $6750 < C_6 < 6950 \text{ a.u.}$ , a

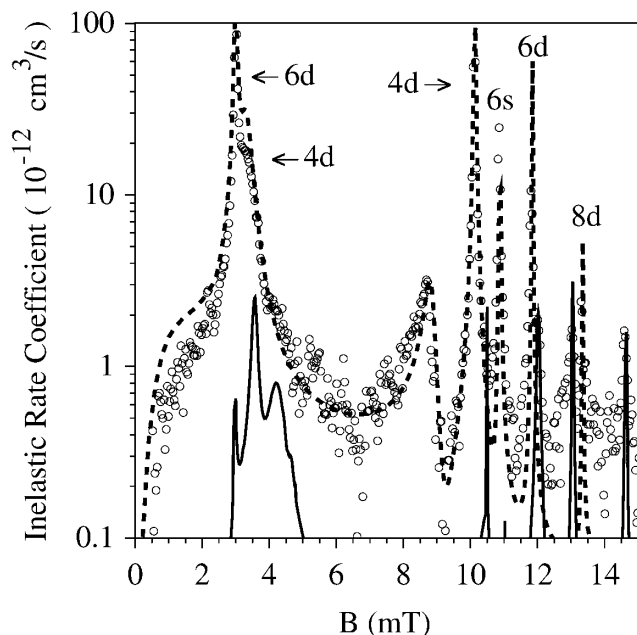


FIG. 2. Inelastic rate for  $(3, -3) + (3, -3)$  collisions (---) and  $(3, -3) + (3, -2)$  collisions (—) for  $C_6 = 6890 \text{ a.u.}$ ,  $S_C = 3.2$ , and  $E/k_B = 5.3 \mu\text{K}$  compared with experiment ( $\circ$ ). Experimental results are scaled by 2.5 (an overall scaling of up to 3 is allowed due to uncertainties in the atom density).

new fit point ( $a_T', a_S', S_C$ ) could be located to an accuracy of 0.05% using the following simple linear relations for the scaled scattering lengths:

$$\begin{aligned} A_T^s &= 3.03628 \times 10^{-4} C_6 + 3.06554, \\ A_S^s &= 0.336475 A_T^s + 0.45426. \end{aligned} \quad (1)$$

The large uncertainties in  $C_6$  arise because the magnetic field positions of the resonances that belong to collision between  $f_a = 3$  and  $f_b = 3$  atoms are determined predominantly by the structure of the Hamiltonian and the Hamiltonian's magnetic field dependency.  $C_6$  can be constrained by fitting the  $(4, -4) + (4, -4)$   $8d$  inelastic resonance at  $20.5029 \pm 0.0040 \text{ mT}$  [1]. The  $8s$  entrance channel lies 18 GHz above the  $f_a = f_b = 3$  asymptote and the  $8d$  resonance position is sensitive only to  $C_6$ ,  $a_T$ , and the already constrained value of  $S_C$ . By restricting  $a_T$  using Eq. (1) we can vary  $C_6$  and  $B$  to determine at which  $C_6$  a resonance occurs at  $20.5029 \text{ mT}$  in the  $(4, -4) + (4, -4)$  inelastic rate. This fit gives  $C_6 = 6890 \pm 2 \text{ a.u.}$  with  $a_T = (2405 \pm 50)a_0$ ,  $a_S = (280.3 \pm 0.3)a_0$ , and  $S_C = 3.2 \pm 0.05$ . Sensitivity of this fit to  $C_8$  and  $V_{\text{ex}}$  is described below.

These model parameters predict the shapes and positions of more than 30 observed Feshbach resonances [1] without additional fitting. A portion of these are depicted in Fig. 2. The resonances include those observed in collisions between  $(4, m_a) + (4, m_b)$ ,  $(4, m_a) + (3, m_b)$ , and  $(3, m_a) + (3, m_b)$  atoms with  $m_a = m_b$  or  $m_a \neq m_b$  that occur for both  $s$ - and  $p$ -wave entrance channels and  $s$ -,  $p$ -,  $d$ -, and  $f$ -wave exit channels.

The modeling performed so tightly constrains the scattering lengths and  $C_6$  that investigation of effects due to the detailed shape of the interaction potential and its long range form is warranted. This analysis included a *flattened potential* case where the  $X^1\Sigma_g^+$  and  $a^3\Sigma_u$  potentials in the range  $8 \rightarrow 9.5a_0$  and  $10 \rightarrow 2a_0$ , respectively, were set to a constant equal to their maximum depth. This severe distortion added several new bound states to each potential. Furthermore, Ref. [11] found that inelastic rates are dominated by the magnitude of the second-order spin-orbit interaction at the zero-energy inner turning point  $R_{\text{in}}$  of the  $a^3\Sigma_u$  potential which then affects the value of  $S_C$ . We tested  $R_{\text{in}}$  in the range  $9.767a_0$  to  $10.496a_0$  which is larger than its expected uncertainty estimated from the *ab initio* calculation of Stevens as  $(10.01 \pm 0.1)a_0$  and should provide extrema for the uncertainties induced in the scattering parameters. The unmodified potential for  $C_6 = 6890 \text{ a.u.}$  has  $R_{\text{in}} = 10.093a_0$ . We investigated the uncertainty due to  $C_8$  by increasing its magnitude by 10%, which is larger than the 5% variation typically found in the literature [15,16,19]. The shape of  $V_{\text{ex}}$  was also altered using the form in Ref. [19]. Finally retardation was removed.

From this detailed error analysis, where we repeated our fitting procedure in each case, we conclude that the combined standard uncertainties in the scattering parameters

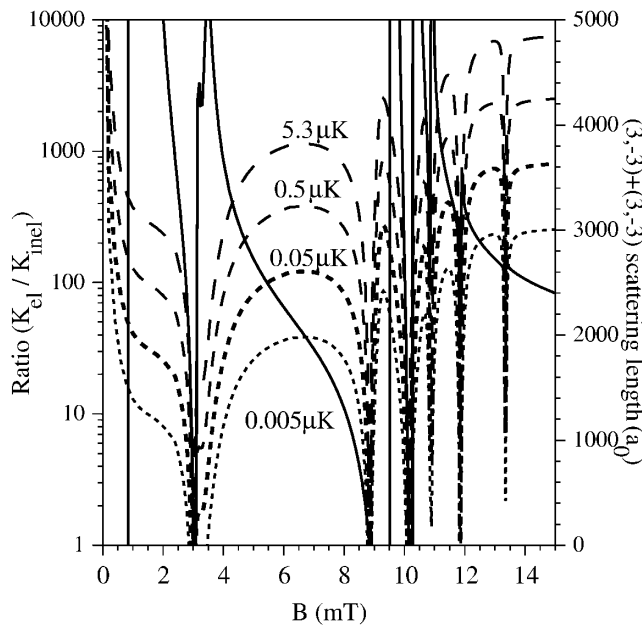


FIG. 3. Dashed lines denote the collision ratio  $K_{el}/K_{inel}$  for  $(3, -3) + (3, -3)$  atoms and the solid line positive scattering lengths.

for  $^{133}\text{Cs}$  are  $a_T = (2400 \pm 100)a_0$ ,  $a_S = (280 \pm 10)a_0$ ,  $C_6 = 6890 \pm 35$  a.u., and  $S_C = 3.2_{-2}^{+1.1}$ . Using only Eq. (1) with  $C_6 = 6890 \pm 35$  a.u. provides erroneously large uncertainties in  $a_T$  and  $a_S$  since the model parameters are correlated in a complicated manner not described by this equation. The 10% change in  $C_8$  caused the largest uncertainties of the fitted parameters. A more accurate value for  $C_8$  would further constrain  $a_T$ ,  $a_S$ , and  $C_6$ . Observation of Feshbach resonances in different isotopes of Cs would allow us to constrain the number of bound states in the  $X^1\Sigma_g^+$  and  $a^3\Sigma_u$  potentials.

Furthermore, the error estimate for  $S_C$  has been grossly exaggerated by the very large variations used for  $R_{in}$ . Given the uncertainty in  $R_{in}$  from [13] we estimate a value of  $S_C = 3.2 \pm 0.5$  is appropriate. These small uncertainties in our model parameters  $a_T$ ,  $a_S$ ,  $C_6$ , and  $S_C$  indicate that we should be able to predict the position of Feshbach resonances to better than 0.05 mT. Finally, we note that our fitted value of  $C_6$  is in excellent agreement with the recent value of  $6851 \pm 74$  a.u. calculated in Ref. [18].

Our results have been compared with previous Cs experimental data including those reported in Refs. [4–10] and the photoassociation data analyzed in [3] and are consistent with these experiments [20]. Calculations of Cs fountain clock shifts based on the current results predict a change in sign of the clock shift near  $0.1 \mu\text{K}$ . This zero in the pressure shift may have important implications in improving the accuracy of Cs fountain clocks. We plan to use this accurate model of Cs ground states interactions to search for confinement effects of Cs atoms in optical lattices, which may be relevant to schemes for quantum computing with neutral atoms.

Our calculations predict the  $(4, 4) + (4, 4)$  scattering length is  $(2400 \pm 100)a_0$ ; however, BEC is inhibited by the large inelastic rates also observed by Refs. [4,5]. For  $B < 0.8$  mT where attempts at BEC with  $(3, -3)$  atoms have been made [5,7] we predict the  $(3, -3) + (3, -3)$  scattering length is negative with a value of  $(-2770 \pm 120)a_0$  at  $B = 0$  which increases in magnitude as  $B$  increases to 0.8 mT. In Fig. 3 we show regions where the  $(3, -3) + (3, -3)$  scattering length is positive and show the ratio of the elastic  $K_{el}$  to the inelastic  $K_{inel}$  rate coefficients ( $K_{el}/K_{inel}$ ) as an estimate of the evaporative cooling efficiency at various temperatures. In regions where the ratio is largest the scattering lengths are typically  $>2000a_0$  and elastic rate coefficients are of the order  $5 \times 10^{-10}$  to  $5 \times 10^{-9}$   $\text{cm}^3/\text{s}$  at all temperatures.

We find that all  $B = 0$  scattering lengths for collisions between  $f_a = 4 + f_b = 4$  or 3 atoms are *positive* with magnitudes typically greater than  $1000a_0$  and all  $f_a = 3 + f_b = 3$  lengths are negative and  $>2770a_0$ . The large magnitude of the Cs scattering lengths has a complicated analysis of Cs, since a constant elastic cross section appropriate to the Wigner-law regime is reached only at temperatures  $T \ll 1 \mu\text{K}$ . Additional details and their relevance to future experiments will be the subject of a future publication [21].

- [1] C. Chin *et al.*, preceding Letter, Phys. Rev. Lett. **85**, 2717 (2000).
- [2] S. J. J. M. F. Kokkelmans *et al.*, Phys. Rev. Lett. **81**, 951 (1998).
- [3] C. Drag *et al.*, Phys. Rev. Lett. **85**, 1408 (2000).
- [4] M. Arndt *et al.*, Phys. Rev. Lett. **79**, 625 (1997).
- [5] J. Söding *et al.*, Phys. Rev. Lett. **80**, 1869 (1998).
- [6] D. Guéry-Odelin *et al.*, Europhys. Lett. **1**, 25 (1998).
- [7] S. A. Hopkins *et al.*, Phys. Rev. A **61**, 032707 (2000).
- [8] V. Vuletić *et al.*, Phys. Rev. Lett. **82**, 1406 (1999).
- [9] R. Legere and K. Gibble, Phys. Rev. Lett. **81**, 5780 (1998); K. Gibble and S. Chu, Phys. Rev. Lett. **70**, 1771 (1993); B. J. Verhaar, K. Gibble, and S. Chu, Phys. Rev. A **48**, R3429 (1993).
- [10] S. Ghezali *et al.*, Europhys. Lett. **36**, 25 (1996).
- [11] P. J. Leo *et al.*, Phys. Rev. Lett. **81**, 1389 (1998).
- [12] F. Mies *et al.*, J. Res. Natl. Inst. Stand. Technol. **101**, 521 (1996).
- [13] M. Krauss and W. J. Stevens, J. Chem. Phys. **93**, 4236 (1990).
- [14] K. T. Tang, J. P. Toennies, and C. L. Yiu, Int. Rev. Phys. Chem. **17**, 363 (1998).
- [15] M. Marinescu, J. F. Babb, and A. Dalgarno, Phys. Rev. A **50**, 3096 (1994).
- [16] S. H. Patil and K. T. Tang, J. Chem. Phys. **106**, 2301 (1997).
- [17] M. Marinescu and A. Dalgarno, Phys. Rev. A **52**, 311 (1995).
- [18] A. Derevianko *et al.*, Phys. Rev. Lett. **82**, 3589 (1999).
- [19] W. Weickenmeier *et al.*, J. Chem. Phys. **82**, 5354 (1985).
- [20] J. P. Burke and P. J. Leo (private communication).
- [21] P. J. Leo *et al.* (to be published).